

# Promoter–enhancer looping at the PPAR $\gamma$ 2 locus during adipogenic differentiation requires the Prmt5 methyltransferase

Scott E. LeBlanc<sup>1</sup>, Qiong Wu<sup>1</sup>, Pallavi Lamba<sup>1</sup>, Saïd Sif<sup>2,3</sup> and Anthony N. Imbalzano<sup>1,\*</sup>

<sup>1</sup>Department of Cell and Developmental Biology, University of Massachusetts Medical School, 55 Lake Avenue North, Worcester, MA 01655, USA, <sup>2</sup>Department of Biological and Environmental Sciences, College of Arts and Sciences, Qatar University, P.O. Box 2713, Doha, Qatar and <sup>3</sup>Department of Internal Medicine, The Ohio State University College of Medicine, 395 W. 12th Avenue, Third Floor, Columbus, OH 43210, USA

Received August 8, 2015; Revised February 5, 2016; Accepted February 22, 2016

## ABSTRACT

PPAR $\gamma$ 2 is a critical lineage-determining transcription factor that is essential for adipogenic differentiation. Here we report characterization of the three-dimensional structure of the PPAR $\gamma$ 2 locus after the onset of adipogenic differentiation and the mechanisms by which it forms. We identified a differentiation-dependent loop between the PPAR $\gamma$ 2 promoter and an enhancer sequence 10 kb upstream that forms at the onset of PPAR $\gamma$ 2 expression. The arginine methyltransferase Prmt5 was required for loop formation, and overexpression of Prmt5 resulted in premature loop formation and earlier onset of PPAR $\gamma$ 2 expression. Kinetic studies of regulatory factor interactions at the PPAR $\gamma$ 2 promoter and enhancer revealed enhanced interaction of Prmt5 with the promoter that preceded stable association of Prmt5 with enhancer sequences. Prmt5 knockdown prevented binding of both MED1, a subunit of Mediator complex that facilitates enhancer–promoter interactions, and Brg1, the ATPase of the mammalian SWI/SNF chromatin remodeling enzyme required for PPAR $\gamma$ 2 activation and adipogenic differentiation. The data indicate a dynamic association of Prmt5 with the regulatory sequences of the PPAR $\gamma$ 2 gene that facilitates differentiation-dependent, three-dimensional organization of the locus. In addition, other differentiation-specific, long-range chromatin interactions showed Prmt5-dependence, indicating a more general role for Prmt5 in mediating higher-order chromatin connections in differentiating adipocytes.

## INTRODUCTION

In addition to being a primary storage site for excess fat, adipose tissue is an active endocrine organ that produces multiple secreted factors such as adipokines that influence signaling, metabolism and the immune system. Obesity changes the generation and release of adipokines such that obese adipose tissue produces inflammatory cytokines involved in the initiation and development of metabolic syndromes including insulin resistance, diabetes and cardiovascular diseases (1). Many molecular mechanisms have been identified in adipocyte differentiation using *in vitro* adipocyte models. The developmental process from adipocyte precursors (pre-adipocytes) to adipocytes is controlled by an array of transcription factors, most notably the master regulator peroxisome proliferator-activated receptor  $\gamma$ 2 (PPAR $\gamma$ 2) that directs adipocyte gene expression in conjunction with CCAAT/enhancer-binding protein- $\alpha$  (C/EBP $\alpha$ ) (2). Prior to the induction of these critical lineage determining factors, the early transcription factor C/EBP $\beta$  marks hotspots where multiple factors converge in the same genomic region in a stretch of  $\sim$ 400 bp on adipogenic genes, leading to changes in epigenetic marks and alterations in chromatin structure (3,4).

Such hotspots are not restricted to the promoters of adipogenic genes. Indeed, they can be observed at more distal regions. These enhancer sequences have been proposed to act through DNA looping (5–7) to bring these elements closer to the promoters to influence adipogenic gene expression. One such potential enhancer is located 10 kb upstream relative to the transcription start site (TSS) of PPAR $\gamma$ 2. First identified as a region that showed dynamic changes in H3K9 acetylation and C/EBP $\alpha$  binding (8), this sequence has also been established as having increased levels of DNase hypersensitivity (9), H3K27 acetylation, H3K4 mono and di-methylation, and Pol II binding as a function of adipogenesis (10). With respect to transcription factor binding, multiple transcription factors, including C/EBP $\beta$ ,

\*To whom correspondence should be addressed. Tel: +1 508 856 1029; Fax: +1 508 856 5612; Email: Anthony.imbalzano@umassmed.edu

C/EBP $\delta$ , MLL4, KLFs and STATs, converge on this element early upon induction of adipogenesis (11).

While extensive research has examined the role of lysine modifications with respect to the control of gene expression in adipogenesis, the impact of arginine post-translational writers is less well characterized. Protein arginine methyltransferase 5 (Prmt5) is an arginine methyltransferase that symmetrically di-methylates arginine residues on histone H2AR3 (12) as well as H4R3 (13) and H3R8 (14). In addition, it methylates non-histone proteins involved in RNA processing, DNA damage, cell cycle regulation and cancer (15). Prmt5 has been shown to be required for both myogenesis (16,17) and adipogenesis (18). Our prior work showed that it is necessary for the expression of late adipocyte-specific genes because it facilitates binding of adenosine triphosphate (ATP)-dependent chromatin remodeling enzymes and for the auto-regulatory process driving the expression of PPAR $\gamma$ 2. At the end point of differentiation, Prmt5 binds to the  $-10$  kb region of the PPAR $\gamma$ 2 locus and, when overexpressed, facilitates earlier adipogenic differentiation (18). However, the exact mechanism by which Prmt5 drives adipogenesis, in particular with respect to PPAR $\gamma$ 2 induction, is unknown.

Our current study shows that Prmt5 is necessary for a differentiation-dependent DNA looping interaction between the PPAR $\gamma$ 2 promoter and the  $-10$  kb region. As a function of differentiation, binding of Prmt5 transitions from binding at the PPAR $\gamma$ 2 promoter to the upstream enhancer. This transition occurs prior to the formation of the loop, and the onset of looping tracks with PPAR $\gamma$ 2 expression. Prmt5 was required for the recruitment of MED1 and Brg1 to both the PPAR $\gamma$ 2 promoter as well as the  $-10$  kb enhancer. Overexpression of Prmt5 facilitated earlier binding of MED1 to the promoter and PPAR $\gamma$ 2 expression was induced earlier and to a greater extent. Taken together these findings suggest a novel role for Prmt5 in adipogenesis in facilitating an enhancer–promoter loop to promote expression of a lineage-determining transcription factor and subsequent adipogenic differentiation. Additional findings indicate that Prmt5 is also required for the formation of other long-range, differentiation-dependent chromatin interactions, suggesting a more general role for Prmt5 in high-order chromatin organization.

## MATERIALS AND METHODS

### Chromosome conformation capture (3C)

The 3C assay was adapted from published methods with revisions (19–21). C3H10T1/2 plates were cross-linked in 1% formaldehyde for 5 min and quenched in 0.125 M glycine. Samples were pelleted and resuspended with lysis buffer (10 mM Tris HCl pH 8.0, 10 mM NaCl, 0.5% NP-40 and protease inhibitor cocktail (Sigma-Aldrich, St Louis, MO, USA), homogenized by douncing, and washed and resuspended in 1 ml of NEB buffer CutSmart. Ten 100- $\mu$ l aliquots were taken. A total of 262  $\mu$ l of Cutsmart buffer was added to each, followed by 38  $\mu$ l of 1% sodium dodecyl sulphate (SDS) and samples were heated for 10 min at 65°C. SDS was then quenched by addition of 44  $\mu$ l of 10% Triton X-100. Each aliquot of lysate was digested with

400 units of restriction enzymes StuI and PvuII and incubated overnight at 37°C. The restriction enzymes were inactivated by addition of 10% SDS to a final concentration of 1.6% (86  $\mu$ l) for 30 min at 65°C. The digested samples were then treated with a ligation cocktail containing 745  $\mu$ l of 10% Triton X-100, 745  $\mu$ l of 10 $\times$  ligation buffer (500 mM Tris–HCl pH7.5, 100 mM MgCl<sub>2</sub> and 100 mM DTT), 80  $\mu$ l of 10 mg/ml bovine serum albumin, 80  $\mu$ l of 100 mM ATP and water to bring the total volume to 7.6 ml. Each aliquot was then ligated with 5000 U of T4 DNA ligase for 4 h at 16°C. Cross-linked DNA was reversed by proteinase K (20 mg/ml) and RNase A (10 mg/ml) overnight. All ligated samples for each sample were then pooled and purified with either a phenol/chloroform extraction followed by ethanol precipitation or with the DNeasy Blood and Tissue kit (Qiagen). Purified DNA samples were analyzed by realtime polymerase chain reaction (PCR) using a standard curve on the ABI StepOne Plus (Applied Biosystems, Foster City, CA, USA) and interaction frequencies were normalized to the values of intra-genic interactions occurring at the endogenous TFIIH (ERCC3) locus (22). The interaction frequency was calculated as the ratio of ligated products to the corresponding frequency of random ligation of the product from the digested bacterial artificial chromosome (BAC) encoding the mouse PPAR $\gamma$  locus (RP24–163B22) as described (23). Primers for 3C experiments are listed in Supplemental Table S1 or were published previously (23).

### Cell culture

Proliferating C3H10T1/2 mesenchymal stem cells and 3T3-L1 cells were maintained in 10% fetal calf serum (FCS). For adipogenic differentiation, 2 day post-confluent cells were differentiated using a standard adipogenic cocktail (1  $\mu$ g/ml insulin, 0.25  $\mu$ g/ml dexamethasone, 0.5 mM IBMX, with 10% FCS). The cocktail for differentiating C3H10T1/2 cells also included 10  $\mu$ M troglitazone. After 48 h, cells were maintained in medium containing 1  $\mu$ g/ml insulin until harvest. Retroviruses encoding Prmt5 or antisense Prmt5 (14,24) were generated in Bosc23 cells (25).

### siRNA

Prior to transfection, cells were grown in antibiotic free medium. Cells were transfected at 60–70% confluence using the Lipofectamine 2000 (Invitrogen) reagent with 40 nM siRNA (scrambled, MED1 or Prmt5) for 6 h with replacement of growth media. C/EBP $\alpha$  knockdown was accomplished with Mm Cebpa 1 FlexiTube siRNA or Mm Cebpa 2 FlexiTube siRNA (Qiagen) under the same conditions. Forty-eight hours after transfection, the cells were induced to differentiate. The cells were harvested for chromatin immunoprecipitation (ChIP), protein and Oil Red O staining at the indicated time points. siRNA sequences are listed in Supplemental Table S1.

### Oil Red O staining

The differentiating cells were fixed with 10% phosphate-buffered formalin for 1 h. The cells were washed with phosphate buffered saline (PBS) and 60% isopropanol twice. The

cells were then stained with a working solution of 60% Oil Red O (60:40 stain-water) for 1 h and washed repeatedly with water to remove excess Oil Red O.

### Reporter assays

A fragment containing the  $-10$  kb region was amplified from mouse genomic DNA and inserted into the KpnI site of a pGL3-basic luciferase plasmid (Promega, Madison, WI, USA) that contains 1.6 kb of the promoter for PPAR $\gamma$ 2. Plasmids were screened for orientation and verified by restriction digest and sequencing by GeneWiz. Luciferase assays were performed using the Dual-Glo Luciferase Assay System (Promega) on the Glo/Max luminometer. Primer sequences are listed in Supplemental Table S1.

### RNA isolation and analysis

RNA was purified using the TRIzol reagent (Invitrogen), and quantitative reverse transcription-PCR was performed as described previously (18). The relative amounts of PPAR $\gamma$ 2 were determined using the comparative threshold cycle method (26) and normalized to the relative levels of cyclophilin B mRNA. Primer sequences are listed in Supplemental Table S1.

### Chromatin immunoprecipitation (ChIP) and Re-ChIP assays

ChIP assays on samples harvested from C3H10T1/2 cells under the listed conditions at the specified time points were performed as described previously (18). Samples were cross-linked in 1% formaldehyde and quenched with 0.125 M glycine. Samples were then lysed in a buffer [1% sodium dodecyl sulfate (SDS), 10 mM ethylenediaminetetraacetic acid (EDTA), 50 mM Tris-HCl (pH 8.1)] containing protease inhibitors (Roche eComplete tablet) and sonicated in a Bio-Ruptor (Diagenode) to 500 bp. A total of 100  $\mu$ g of sonicated lysates were diluted in immunoprecipitation dilution buffer [0.01% SDS, 1.1% Triton X-100, 1.2 mM EDTA, 16.7 mM Tris (pH 8.1), 167 mM NaCl] containing protease inhibitors (Sigma-Aldrich, St Louis, MO, USA). Antibodies were then added to lysates and the combined antibody/DNA complexes were incubated with Magna-ChIP A/G beads (EMD Millipore) overnight at 4°. Beads were washed in low salt [0.1% SDS, 1% Triton X-100, 2 mM EDTA, 20 mM Tris-HCl (pH 8.1), 150 mM NaCl], once in high salt buffer (same buffer containing 500 mM NaCl), followed by LiCl buffer [0.25 M LiCl, 1% Nonidet P-40, 1% sodium deoxycholate, 1 mM EDTA, 10 mM Tris-HCl (pH 8.1)] and finally were washed with Tris-EDTA (pH 8.0). Complexes were released from the beads using elution buffer [1% SDS 0.1M NaHCO<sub>3</sub> with Proteinase K for 2 h while shaking at 62°C. The samples were purified with the Zymo ChIP purification kit (Zymo). Either polyclonal rabbit antisera against Prmt5 (24) and Brg1 (27) and purified antibodies against MED1 (Bethyl Labs, Montgomery, TX, USA) or normal rabbit IgG (Millipore Corp., Bedford, MA, USA) were used. Purified DNA was analyzed by quantitative real-time PCR. Primer sequences are listed in Supplemental Table S1.

For re-ChIP, after washing as described above, the immune complexes were eluted in 50  $\mu$ l for 10 min at room temperature, and this was repeated twice to obtain 150  $\mu$ l in total. A total of 75  $\mu$ l of this eluate was decrosslinked, purified and analyzed by quantitative real-time PCR directly (first round ChIP only), and the remaining 75  $\mu$ l was diluted to a final volume of 750  $\mu$ l using ChIP dilution buffer without SDS. After addition of the second-round ChIP antibody, the samples were incubated overnight at 4°C and treated as described above. Elution was performed as described for the first-round re-ChIP and the eluate was decrosslinked, purified and analyzed by quantitative real-time PCR.

### Protein analysis

Day 0 and day 6 C3H10T1/2 10-cm plates were scraped into 1 ml of PBS. The cell pellets were snap frozen in liquid N<sub>2</sub> and stored at  $-80$  °C. The pellets were resuspended in 200  $\mu$ l of lysis buffer containing 50 mM Tris-HCl (pH 7.5), 150 mM NaCl, 0.5% Nonidet P-40 and 20% glycerol, along with Sigma protease inhibitor cocktail. After sonication, the protein amounts were quantified using a Bradford assay. Protein (50  $\mu$ g) was loaded on an sodium dodecyl sulphate-polyacrylamide gel electrophoresis gel and transferred to a nitrocellulose membrane. Primary antibodies were Prmt5 (Santa Cruz; sc-22132), GAPDH (Sigma G9295), MED1 (Bethyl A300-793), C/EBP $\alpha$  (Santa Cruz, sc-9314) and p85 phosphatidylinositol-3-kinase (PI3K; Millipore ABS234). Bands were detected by secondary conjugated horseradish peroxidase antibodies and enhanced chemiluminescence detection.

## RESULTS

### C/EBP $\alpha$ activates the $-10$ kb enhancer upstream of the PPAR $\gamma$ 2 promoter

In addition to the histone modifiers, transcriptional regulators and DNase hypersensitivity at the  $-10$  kb enhancer (8–10), it has been shown to be bound by C/EBP $\alpha$  in differentiated adipocytes and activates a reporter in response to differentiation of 3T3-L1 cells (8). Cycling C3H10T1/2 cells were transfected with a luciferase reporter construct containing a fragment of the  $-10$ -kb upstream region fused to 1.6 kb of the PPAR $\gamma$ 2 promoter in the presence of increasing amounts of C/EBP $\alpha$  plasmid. At the maximal activation amount of 100 ng, C/EBP $\alpha$  activated the promoter construct 4-fold and activated the promoter and enhancer construct 14-fold (Supplemental Figure S1). C/EBP $\alpha$  levels produced at 200 and 400 ng of transfected plasmid exhibited reductions in activation (Supplemental Figure S1), likely due to squelching (28). These results serve as a corroboration of the enhancer properties of the  $-10$  kb region with respect to C/EBP $\alpha$ -mediated activation.

### Adipogenic differentiation alters the chromatin landscape at the PPAR $\gamma$ 2 locus

Although enhancers for genes may be distant to the genes they influence, much research has focused on the DNA looping between promoters and enhancers to target the

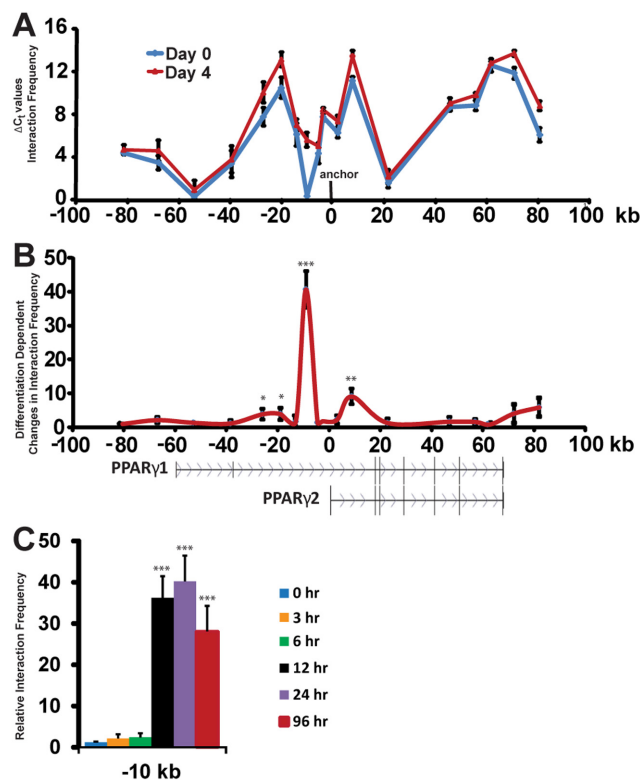


**Figure 1.** 3C analysis of regions 80 kb upstream and downstream of the PPAR $\gamma$  TSS. (A) 3C analysis of the PPAR $\gamma$  locus in day 0 and day 4 differentiated C3H10T1/2 cells. The positions of the PPAR $\gamma$ 1 and PPAR $\gamma$ 2 genes are diagrammed relative to the x-axis, which indicates the genomic position relative to the PPAR $\gamma$ 2 TSS. The anchor position at the PPAR $\gamma$ 2 promoter is indicated. The interaction frequency was normalized to the value between the promoter and the  $-10$  kb region in day 0 undifferentiated cells; this  $-10$  kb value was set at 0 to show changes in  $\Delta C_i$  values relative to the  $-10$  kb interaction. (B) Relative 3C values from (A) shown to reflect the differences between the differentiated and undifferentiated states. (C) Time course of interaction frequency between the promoter and the  $-10$  kb enhancer sequence. Samples of C3H10T1/2 cells were taken at the 0 h timepoint and at 3, 6, 12, 24 and 96 h following differentiation. All results are from three independent samples performed in triplicate. Error bars: Mean  $\pm$  SD (\* $P$  < 0.05, \*\* $P$  < 0.01, \*\*\* $P$  < 0.001 by Student's two tailed  $t$ -test).

transcriptional apparatus to the region around the start site of transcription (29). While previous studies have examined looping in adipogenesis, thus far they have been restricted to brown fat (30,31) or have focused on the loci encoding uncoupling proteins 2 and 3 (32). We performed chromosome conformation capture (3C) assays (33) to examine the PPAR $\gamma$  locus. Setting the PPAR $\gamma$ 2 promoter as an anchor point, we investigated the interactions between the promoter and different regions of the locus using fragments generated by PvuII and StuI, which generate cleavage fragments that include both the  $-10$  kb enhancer and the proximal promoter region. While the promoter exhibited interactions with many regions of the PPAR $\gamma$ 2 locus in both undifferentiated and differentiated cells (Figure 1A), we noted a  $>40$ -fold differentiation-dependent change in the association of the promoter and the upstream enhancer (Figure 1B). We also observed a statistically significant increase in association between the promoter and a region  $\sim 7$

kb downstream of the PPAR $\gamma$ 2 TSS. This region encompasses a previously identified hotspot that includes a region of DNase I hypersensitivity and binding of 15 transcription factors associated with adipogenic activation at  $\sim +3$  kb (11) and C/EBP $\beta$ , C/EBP $\alpha$  and PPAR $\gamma$ 2 binding at  $+13$  kb (8,9), however, this interaction was not further investigated. Based on the evidence of a differentiation-dependent change in interaction frequency between the  $-10$  kb enhancer and the PPAR $\gamma$ 2 promoter, we examined the kinetics of loop formation. The increase in loop formation occurred at the 12 h time point and the loop persisted throughout differentiation (Figure 1C). We also confirmed the existence of a PPAR $\gamma$ 2 promoter–enhancer loop in differentiating 3T3-L1 cells, a different cell model for adipogenesis. In the 3T3-L1 model, the loop appeared earlier, suggesting minor differences in the kinetics of loop formation in the two different cell lines (Supplemental Figure S2A). These findings show reorganization of the higher order chromatin structure at the PPAR $\gamma$ 2 locus as a function of adipogenic differentiation.

### C/EBP $\alpha$ contributes to formation of the loop at the PPAR $\gamma$ 2 locus

Since C/EBP $\alpha$  binds to the  $-10$  kb enhancer sequence (8) and can activate it (Supplemental Figure S1), we tested whether C/EBP $\alpha$  contributed to loop formation. Knockdown of C/EBP $\alpha$  was achieved by siRNA treatment (Supplemental Figure S3A and B). Assessment of loop formation at 12 h post-differentiation revealed that the frequency of loop formation decreased by about 50% but was well above the observed frequency at the onset of differentiation (Supplemental Figure S3C). We conclude that C/EBP $\alpha$  contributes to loop formation but is not essential.

### Prmt5 governs formation of the loop as well as its timing

Given our previous findings that Prmt5 is necessary for adipogenesis (18), we investigated whether the DNA looping interactions are dependent on Prmt5. A time course of Prmt5 protein expression in differentiating C3H10T1/2 cells was performed; levels were similar at each time point examined (Figure 2A). C3H10T1/2 cells were then infected with an empty retroviral vector, with a retroviral vector encoding a human Prmt5 antisense construct previously used to generate stable fibroblast cell lines that exhibited reduced levels of Prmt5 (14), or with a retroviral vector encoding human Prmt5 to allow us to observe the effects of overexpression. Infected cells were selected by puromycin, grown to confluence and differentiated. Western blot and Oil Red O analysis verified the overexpression and knockdown (Figure 2B). Consistent with prior results (18), Prmt5 reduction blocked adipogenic differentiation and Prmt5 overexpression accelerated differentiation (Figure 2C). Prmt5 reduction blocked the formation of the loop between the promoter and the upstream enhancer of PPAR $\gamma$ 2 (Figure 2D). These results were confirmed in 3T3-L1 cells in which Prmt5 levels were reduced (Supplemental Figure S2B–D), demonstrating the generality of the finding. In contrast, cells overexpressing Prmt5 showed increased interaction frequency at 6 h post-differentiation (Figure 2E), indicating that Prmt5

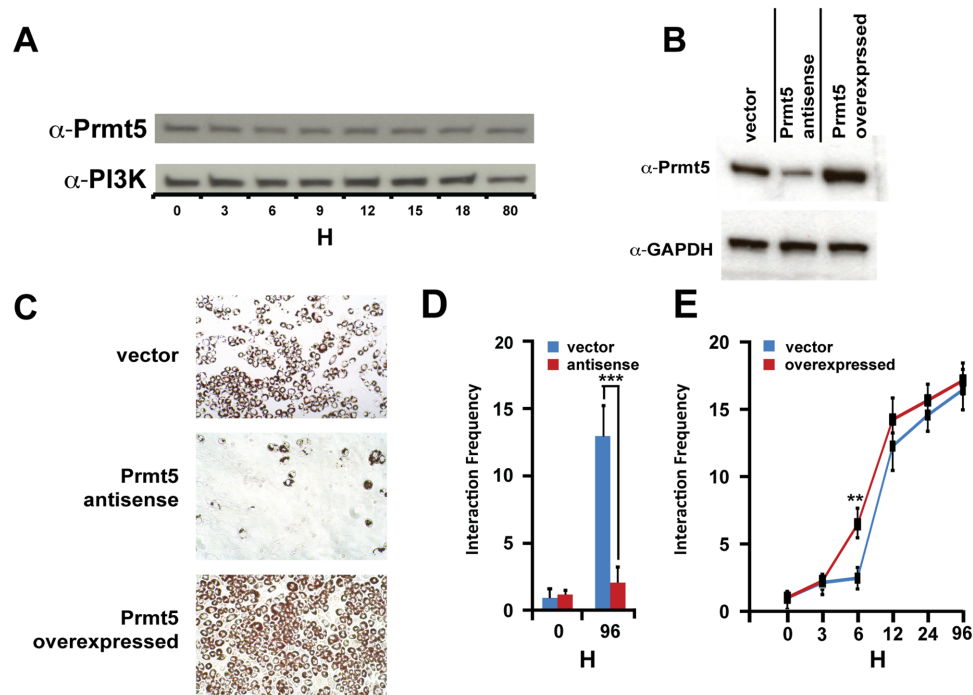


**Figure 2.** Loop formation requires Prmt5. (A) Western blot time course of Prmt5 protein levels over the time course of C3H10T1/2 cells differentiation. PI3K levels were monitored as a control. (B–E) C3H10T1/2 cells were infected with retroviruses containing either a control vector, wild-type Prmt5 or antisense Prmt5. (B) Western blots showing levels of Prmt5 in cells expressing empty vector, antisense and overexpressed Prmt5 96 h post-differentiation. GAPDH levels were monitored as a control. (C) Oil red O staining for cells 4 days post-differentiation. (D) Control vector and antisense Prmt5 expressing cells either collected just prior to differentiation (0 h) or 96 h later were tested by 3C for interactions between the PPAR $\gamma$ 2 promoter and the –10 kb enhancer. (E) Control or cells overexpressing Prmt5 were differentiated for the specified times. Relative interaction frequencies for the interaction between the PPAR $\gamma$ 2 promoter and the –10 kb enhancer were set to the value at the 0 h time point. All results are from three independent samples performed in triplicate. Error bars: Mean + SD (\*\* $P < 0.01$ , \*\*\* $P < 0.001$  by Student's two tailed  $t$ -test).

levels regulate loop formation. There was a decrease in overall interaction frequency compared to uninfected cells (Figure 1), which was attributed to the retroviral infection. Thus, Prmt5 is essential for the formation of the loop and overexpression of Prmt5 can facilitate earlier loop formation.

#### Transition of Prmt5 binding from the PPAR $\gamma$ 2 promoter to the –10 kb enhancer precedes loop formation

To test whether Prmt5 binding plays a role in the formation of the promoter–enhancer loop, we assessed the kinetics of Prmt5 occupancy at the PPAR $\gamma$ 2 promoter or upstream enhancer using ChIP. We previously reported minimal binding for Prmt5 at the PPAR $\gamma$ 2 promoter but rather significant binding at the upstream enhancer at the endpoint of differentiation (18).

The kinetic analysis revealed enhanced Prmt5 occupancy at the PPAR $\gamma$ 2 promoter at 6 h post-differentiation (Figure 3A). In contrast, binding of Prmt5 to the enhancer increased gradually over the time course of differentiation with maximal binding observed at the endpoint (Figure 3A). Overexpression of Prmt5 shifted its occupancy to 3 h post-differentiation at the promoter and elevated binding at the enhancer (Figure 3B), consistent with the earlier formation of the loop (Figure 2E). These results show dynamic binding by Prmt5 at the PPAR $\gamma$ 2 locus prior to loop formation.

#### Loop formation and changes in Prmt5 binding are associated with the onset of PPAR $\gamma$ 2 expression

Given the formation of a loop between the upstream enhancer and the promoter of PPAR $\gamma$ 2 along with the dynamic binding patterns of Prmt5, we tested whether PPAR $\gamma$ 2 expression was related to the differential binding of Prmt5. Prmt5 knockdown was previously shown to prevent upregulation of both PPAR $\gamma$ 2 and adipogenic differentiation (18). Using RNA samples at 3 h intervals from 0 to 18 h, we observed that PPAR $\gamma$ 2 expression was induced above background at the 12 h time point in cells containing the control vector. A significant 2.7-fold increase in mRNA expression was observed at 9 h post-differentiation in cells overexpressing Prmt5 (Figure 3C). In both the control and the cells overexpressing Prmt5, PPAR $\gamma$ 2 mRNA levels continued to increase at the later points as a function of differentiation.

#### MED1 and Brg1 binding at the PPAR $\gamma$ 2 locus

In order to explore the mechanism by which Prmt5 could influence loop formation, we considered two candidates previously shown to be involved in regulating DNA looping, Brg1 and MED1. Brg1, an ATPase of the mammalian SWI/SNF chromatin remodeling complex, has been shown to be necessary for adipogenesis (34), interacts with Prmt5 (14,17) and is required for looping at the  $\alpha$ -globin and  $\beta$ -

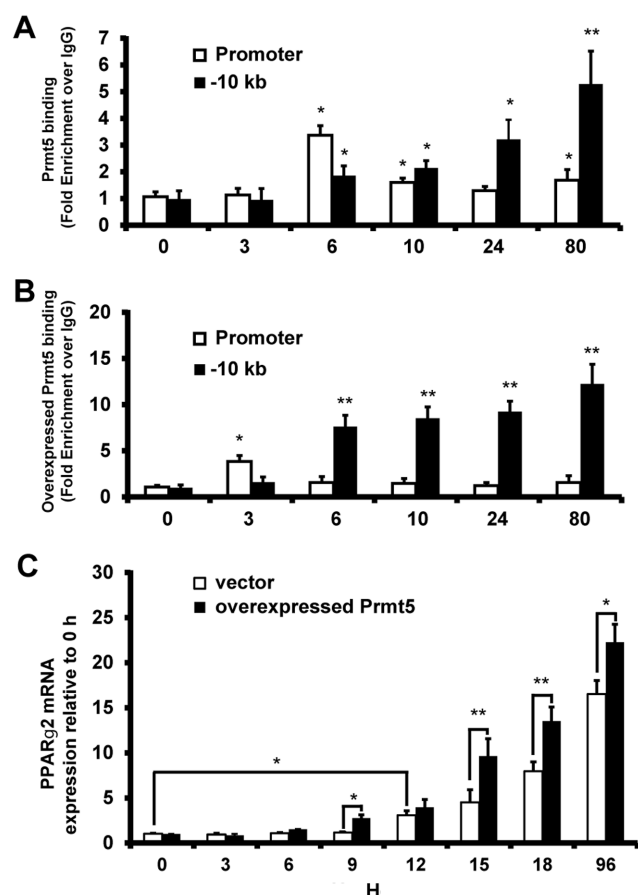


**Figure 3.** Prmt5 binding at the PPAR $\gamma$ 2 enhancer versus the promoter. (A) Samples were collected for ChIP from differentiated C3H10T1/2 cells infected with a retrovirus containing the control vector. (B) Samples were collected for ChIP from differentiated C3H10T1/2 cells infected with a retrovirus for Prmt5 to generate Prmt5 overexpression. (C) Overexpression of Prmt5 resulted in precocious PPAR $\gamma$ 2 expression. RNA samples were taken at the specified time points. The level of PPAR $\gamma$ 2 expression in cells expressing the control empty vector at time 0 was set to 1. Experiments from three independent samples were performed in triplicate and significance is based on values relative to the 0 h time point. (\* $P < 0.05$ , \*\* $P < 0.01$ , by Student's two tailed  $t$ -test).

globin loci during hematopoiesis (35–37) contraction of the IgH locus to establish B cell identity (38), and at the Th2 cytokine and CIITA loci (39,40). MED1, also known as Trap220 or Drip205, is a subunit of the Mediator complex that broadly contributes to transcriptional activation (41). It is required for PPAR $\gamma$ 2 induced adipogenesis (42) and has been shown to interact with PRDM16, the major regulator of brown fat determination (30,31). Previous analyses have documented the binding of MED1 to the PPAR $\gamma$ 2 upstream enhancer as well as to the promoter (8,42) and other work has implicated MED1 in DNA looping (43). Additionally, Prmt5 has been shown to interact with the CDK domains of the Mediator complex (44). At the PPAR $\gamma$ 2 promoter, both Brg1 and MED1 displayed patterns of occupancy with initial binding at 6 h, maximal binding at 12 h and decreased binding as a function of differentiation (Figure 4A). The enhanced binding of Brg1 and MED1 at the PPAR $\gamma$ 2 promoter early in the differentiation pro-

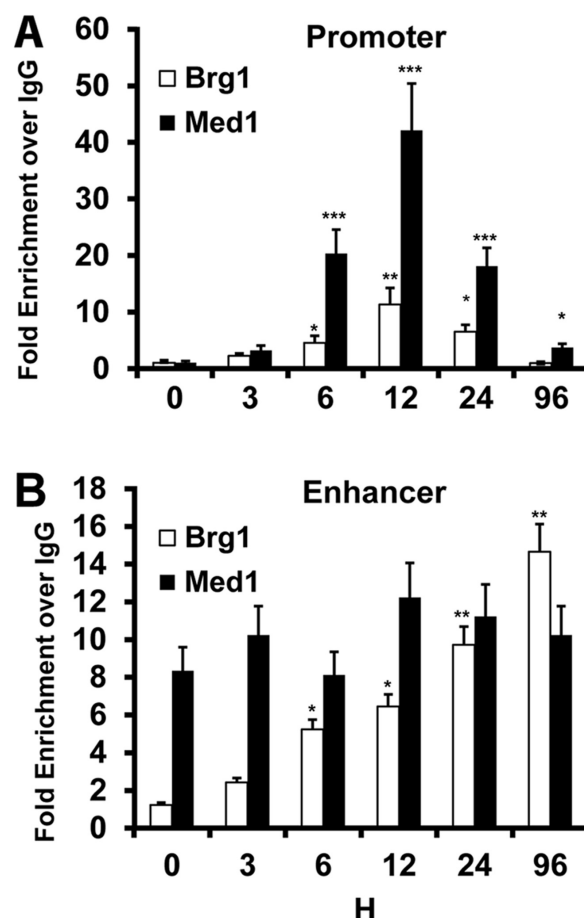


**Figure 4.** MED1 and Brg1 kinetics of binding at the PPAR $\gamma$ 2 locus. ChIP assays for Brg1 and MED1 were performed on 10T1/2 cells differentiated for the indicated times. DNA immunoprecipitated by antibodies against Brg1 and MED1 was amplified and quantified by real-time PCR for the (A) PPAR $\gamma$ 2 promoter or (B) the –10 kb enhancer. Data are presented as fold enrichment over the amount of DNA amplified after immunoprecipitation by the control IgG. All results are from three independent samples performed in triplicate with significance based on values relative to the 0 h time point. Error bars: Mean  $\pm$  SD (\* $P < 0.05$ , \*\* $P < 0.01$ , \*\*\* $P < 0.001$  by Student's two tailed  $t$ -test).

cess mirrors that observed for Prmt5 (Figure 3A). In contrast, occupancy at the –10 kb enhancer showed relatively unchanged levels for MED1, whereas Brg1 occupancy increased as a function of adipogenesis with similar kinetics to Prmt5 (Figure 4B).

#### Prmt5 is required for MED1 and Brg1 binding at the PPAR $\gamma$ 2 locus

We initiated experiments to understand the relationship between the binding of Prmt5, Brg1 and MED1 at the PPAR $\gamma$ 2 locus. Two independent siRNAs for Prmt5 were tested and validated for a block of adipogenesis by Oil Red O staining (Figure 5A–C) as well as reduction in Prmt5 protein level (Figure 5D). Surprisingly, MED1 was recruited in a Prmt5 dependent manner, as Prmt5 depletion prevented MED1 binding at both the promoter and upstream enhancer of PPAR $\gamma$ 2 (Figure 5E). Binding of Brg1 to the promoter and enhancer was also greatly impaired at each time

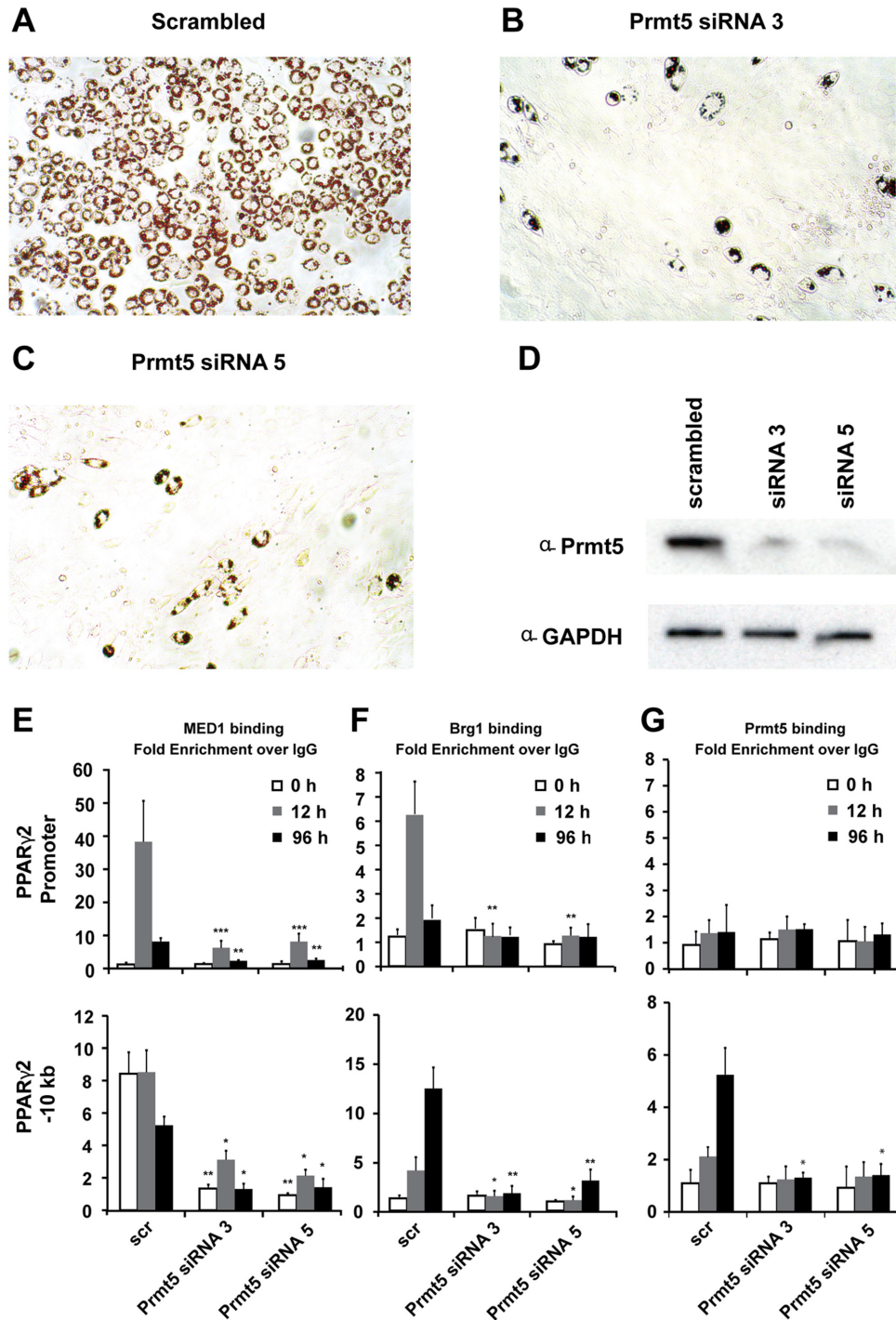


**Figure 5.** Knockdown of Prmt5 blocked binding of Brg1 and MED1 to the PPAR $\gamma$ 2 locus. C3H10T1/2 cells were treated with one of two independent siRNAs for Prmt5 or a scrambled sequence control. (A–C) Oil Red O staining of cells treated with scrambled, Prmt5 siRNA Oligo 3 or Prmt5 siRNA oligo 5. (D) Western demonstrating Prmt5 knockdown. (E–G) Chromatin immunoprecipitation (ChIP) experiments were performed on C3H10T1/2 cells differentiated for 0, 12 and 96 h. DNA was immunoprecipitated with antibodies against (E) MED1, (F) Brg1 or (G) Prmt5. Top panels indicate binding at the PPAR $\gamma$ 2 promoter while bottom panels indicate binding at the –10 kb enhancer. Data are presented as fold enrichment over the amount of DNA amplified after immunoprecipitation by the control IgG. Analysis of three independent samples were performed in triplicate. Error bars: Mean + SD (\* $P$  < 0.05, \*\* $P$  < 0.01, \*\*\* $P$  < 0.001 by Student's  $t$ -test).

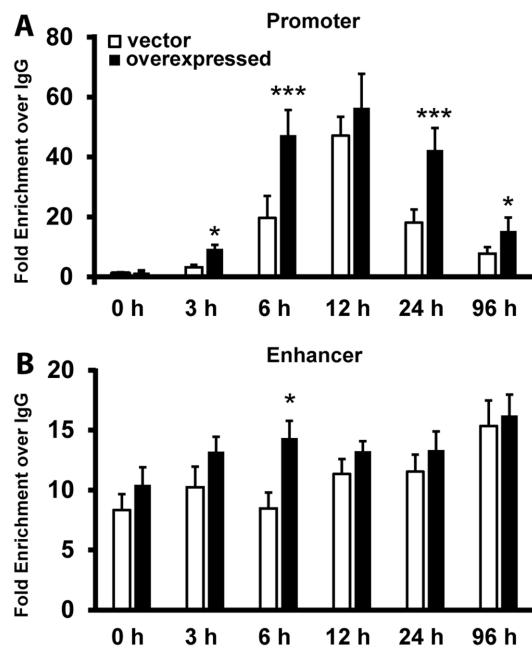


**Figure 6.** Overexpression of Prmt5 results in earlier recruitment of MED1 to the PPAR $\gamma$ 2 promoter. C3H10T1/2 cells were infected with retrovirus containing either empty vector or Prmt5. ChIP experiments for MED1 were performed on cells differentiated for the indicated times. DNA immunoprecipitated by the MED1 antibody was amplified and quantified by real-time PCR for the (A) PPAR $\gamma$ 2 promoter or (B) the  $-10$  kb enhancer. Data are presented as fold enrichment over the amount of DNA amplified after immunoprecipitation by the control IgG. Experiments from three independent samples were performed in triplicate. Error bars: Mean + SD (\* $P$  < 0.05, \*\*\* $P$  < 0.001 by Student's two tailed  $t$ -test).

point (Figure 5F), consistent with our previous observations that knockdown of Prmt5 blocks Brg1 binding at adipogenic target promoters (18). As a control, knockdown of Prmt5 ablated binding of Prmt5 to the upstream enhancer at the 12 and 96 h time points, but showed no effect on promoter binding (Figure 5G). Thus, Prmt5 is needed for the occupancy of both Brg1 and MED1 at both the promoter and upstream enhancer of PPAR $\gamma$ 2.

#### Overexpression of Prmt5 facilitates earlier recruitment of MED1

Given our earlier findings that overexpression of Prmt5 led to more rapid differentiation (18) as well as premature loop formation (Figure 2E), we tested whether the earlier loop formation induced by overexpression of Prmt5 was governed by recruitment of MED1. When overexpressing Prmt5, we observed an earlier and greater occupancy for MED1 at the PPAR $\gamma$ 2 promoter beginning at 3 h, with a robust occupancy seen at 6 h (Figure 6A), which is coincident with the observed early loop formation at the PPAR $\gamma$ 2 promoter (Figure 2E). Enhanced Prmt5 occupancy was observed at the promoter throughout adipogenesis (Figure 6A). At the enhancer where MED1 binding was constitutive, a modest change was observed, most notably at the 6 h time point (Figure 6B). Thus, the earlier loop formation caused by Prmt5 overexpression correlates with premature enhanced binding of MED1.

#### MED1 is required for loop formation and for Brg1 and Prmt5 binding to the PPAR $\gamma$ 2 locus

Given our findings that Prmt5 was necessary for both MED1 and Brg1 to bind, we tested whether the converse was true. In order to address factors that are required for loop formation, we examined the role of Mediator. Two independent siRNAs targeting MED1 blocked differentiation in C3H10T1/2 cells (Figure 7A–C). Control western blots validated the knockdown of MED1 (Figure 7D). 3C studies showed that MED1 knockdown also reduced loop formation at the 12 and 96 h time points (Figure 7E). These results show a necessary role for MED1 in both differentiation and loop formation. Having shown that loss of Prmt5 results in a loss of MED1 and Brg1 to the PPAR $\gamma$ 2 promoter and enhancer, we tested whether MED1 knockdown would influence the binding of Brg1 or Prmt5. Depletion of MED1 blocked binding of MED1 (Figure 8A), of Brg1 (Figure 8B) and of Prmt5 (Figure 8C). Thus, both MED1 and Prmt5 show a mutual requirement for each other in binding to the PPAR $\gamma$ 2 locus.

#### Prmt5 and MED1 co-localize at PPAR $\gamma$ 2 regulatory sequences

The mutual dependence of Prmt5 and MED1 binding suggests but does not prove that both factors are bound together on the same regulatory sequences at the same time. To address this concern, we performed re-ChIP, also called sequential ChIP, experiments. ChIP was performed on cells differentiated for 6 or 96 h with MED1 antibody, and the recovered DNA was prepared for a second ChIP using either Prmt5 antibody or IgG as a control. The reciprocal experiment was also performed. Amplification of DNA recovered from the second ChIP experiments identified the PPAR $\gamma$ 2 promoter sequence at 6 h and to a lesser extent, at 96 h post-differentiation (Figure 9A and B, top panels), in agreement with the enhanced binding of Prmt5 to the promoter at 6 h (Figure 3A). Amplification of DNA recovered from the second ChIP experiments identified the PPAR $\gamma$ 2 enhancer sequence at 96 h post-differentiation (Figure 9A and B, bottom panels). Lower or negligible levels of enhancer sequence were recovered at the 6 h timepoint, as expected based on the enhanced binding of Prmt5 to the PPAR $\gamma$ 2 enhancer at the endpoint of differentiation (Figure 3A). The results indicate co-localization of Prmt5 and MED1 on PPAR $\gamma$ 2 regulatory sequences.

#### Prmt5 is required for other higher-order chromatin interactions in differentiating adipocytes

We next determined whether Prmt5 is involved in other higher-order chromatin interactions that occur in differentiating adipocytes. The uncoupling proteins Ucp2 and 3 are likely involved in mitochondrial function (45–47) but may also play a role in limiting reactive oxygen species formation during respiration (48–50). The genes encoding Ucp2 and Ucp3 are next to each other on mouse chromosome 7 and are separated by  $\sim 20$  kb. Bugge *et al.* previously showed that an intronic enhancer in the Ucp3 gene loops to contact the promoter of the Ucp2 gene in 3T3-L1 cells (32). We

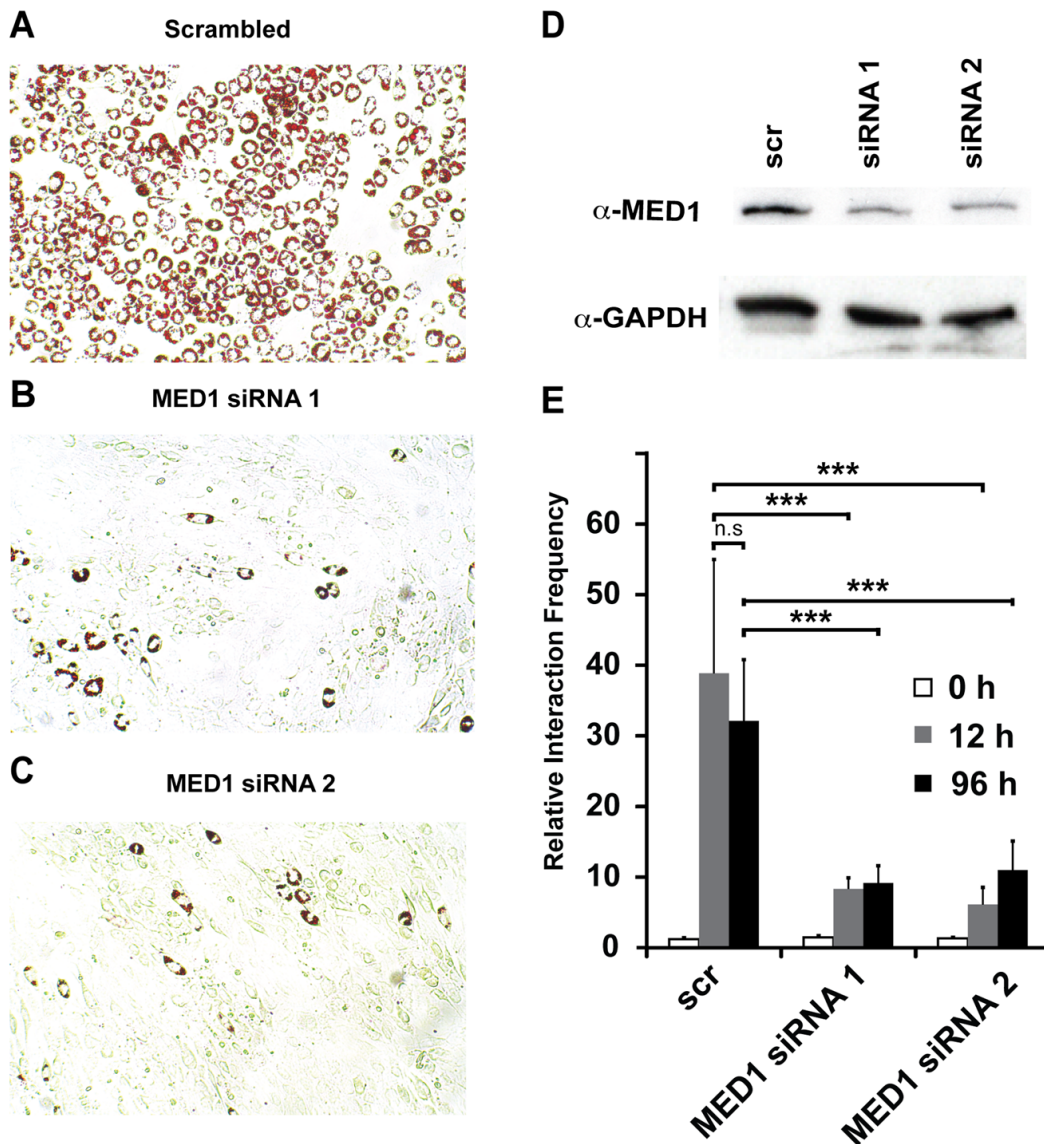


**Figure 7.** MED1 knockdown prevents formation of the loop between the PPAR $\gamma$ 2 -10 kb enhancer and the promoter. C3H10T1/2 cells were treated with scrambled or one of two independent siRNA oligos. (A–C) Oil Red O staining showing inhibition of adipogenesis by siRNA for MED1. (D) Western blot showing MED1 knockdown. (E) Samples were harvested at the 0, 12 and 96 h time points for a 3C assay. Interaction frequency at the 0 h timepoint for the scrambled control was set at 0 and other values are presented relative to that value. Experiments from three independent samples were performed in triplicate. Error bars: Mean + SD (\*\* $P < 0.01$  by Student's two tailed  $t$ -test).

performed 3C experiments over a time course of 3T3-L1 differentiation and identified the existence of the loop at day 4 of the differentiation process (Supplemental Figure S4A), consistent with the published study. The same experiment performed in differentiating C3H10T1/2 cells yielded similar results, with the only difference being a slightly earlier onset of loop formation (Figure 10A). A reduction in Prmt5 levels caused a significantly lower interaction frequency between the Ucp2 and 3 loci in both the C3H10T1/2 (Figure 10B) and the 3T3-L1 cell backgrounds (Supplemental Figure S4B). Ucp2 and 3 are both induced by PPAR $\gamma$  (32), and we have previously shown that knockdown of Prmt5 decreases PPAR $\gamma$ 2 and PPAR $\gamma$ 2 target gene expression while overexpression of Prmt5 increases PPAR $\gamma$ 2 expression (18).

As expected, Ucp2 and Ucp3 mRNA levels were reduced in cells knocked down for Prmt5 in both C3H10T1/2 and 3T3-L1 cells (Figure 10C and Supplemental Figure S4C).

In other previously published work, we determined that the PPAR $\gamma$ 2 promoter makes long-range, transient, contacts with the promoters of several different PPAR $\gamma$  target genes in both 3T3-L1 and C3H10T1/2 cells (23). We examined whether reduction of Prmt5 affected the interaction frequencies between the PPAR $\gamma$ 2 promoter on chromosome 6 and the AdipoQ or perilipin 2 (Plin2) promoters on chromosomes 16 and 4, respectively. The inter-chromosomal interactions were completely Prmt5-dependent. (Figure 10D and E). The data indicate that Prmt5 is not solely required for loop formation at the

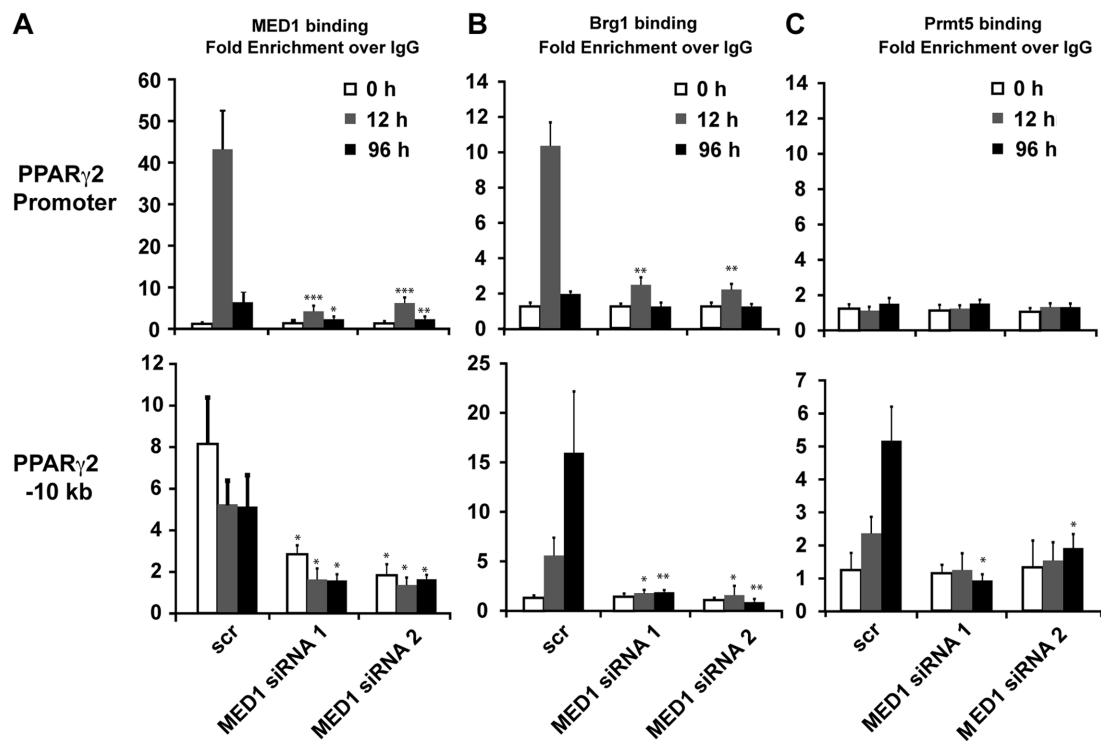


**Figure 8.** Knockdown of MED1 blocked binding of Brg1 and Prmt5 to the PPAR $\gamma$ 2 locus. C3H10T1/2 cells were treated with one of two independent siRNAs for MED1 or a scrambled control siRNA. ChIP experiments were performed on cells differentiated for the indicated times. DNA immunoprecipitated by antibodies against (A) MED1, (B) Brg1 or (C) Prmt5 was amplified and quantified by real-time PCR for the PPAR $\gamma$ 2 promoter (top) and the PPAR $\gamma$ 2 –10 kb enhancer (bottom). Data are presented as fold enrichment over the amount of DNA amplified after immunoprecipitation by the control IgG. Experiments from three independent samples were performed in triplicate. Error bars: Mean + SD (\* $P$  < 0.05, \*\* $P$  < 0.01, \*\*\* $P$  < 0.001 by Student's two tailed  $t$ -test).

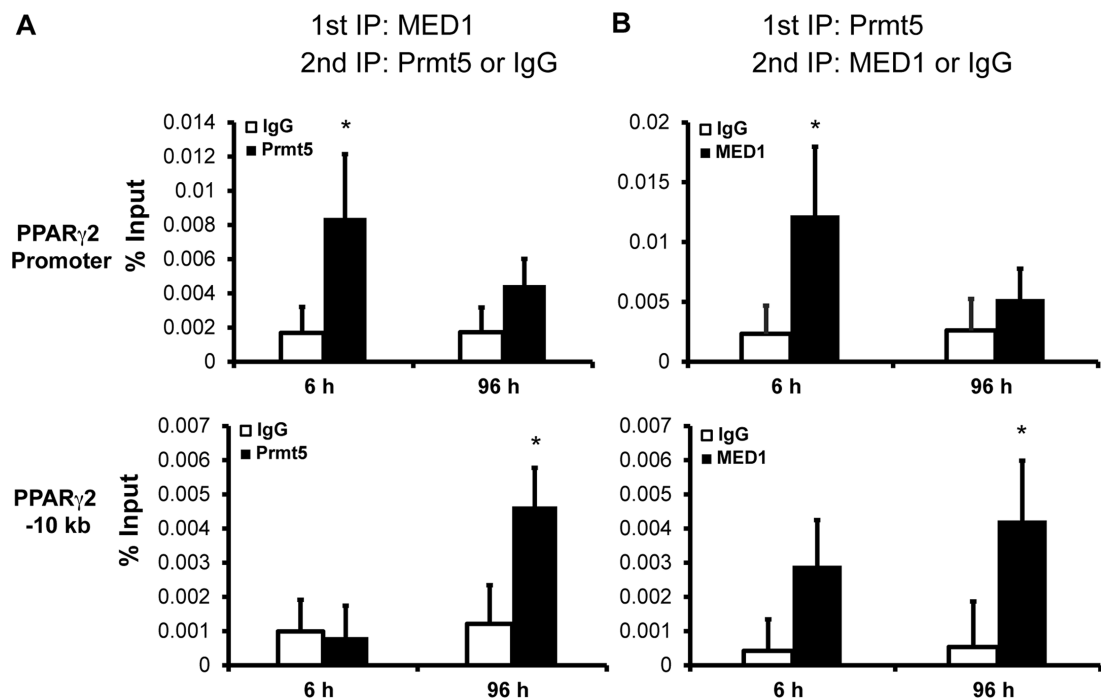


**Figure 9.** MED1 and Prmt5 are co-localized on the same regulatory sequences. Re-ChIP experiments were performed on C3H10T1/2 cells differentiated for 6 or 96 h. (A) Experiments analyzing binding to PPAR $\gamma$ 2 promoter or enhancer sequences using a MED1 antibody followed by either IgG or a Prmt5 antibody for the second ChIP. (B) Experiments analyzing binding to PPAR $\gamma$ 2 promoter or enhancer sequences using a Prmt5 antibody followed by either IgG or a MED1 antibody for the second ChIP. Results are shown as % input rather than relative enhancement to allow better presentation of the IgG control. Experiments from three independent samples were performed in triplicate. Error bars: Mean + SD (\* $P$  < 0.05 by Student's two tailed  $t$ -test).

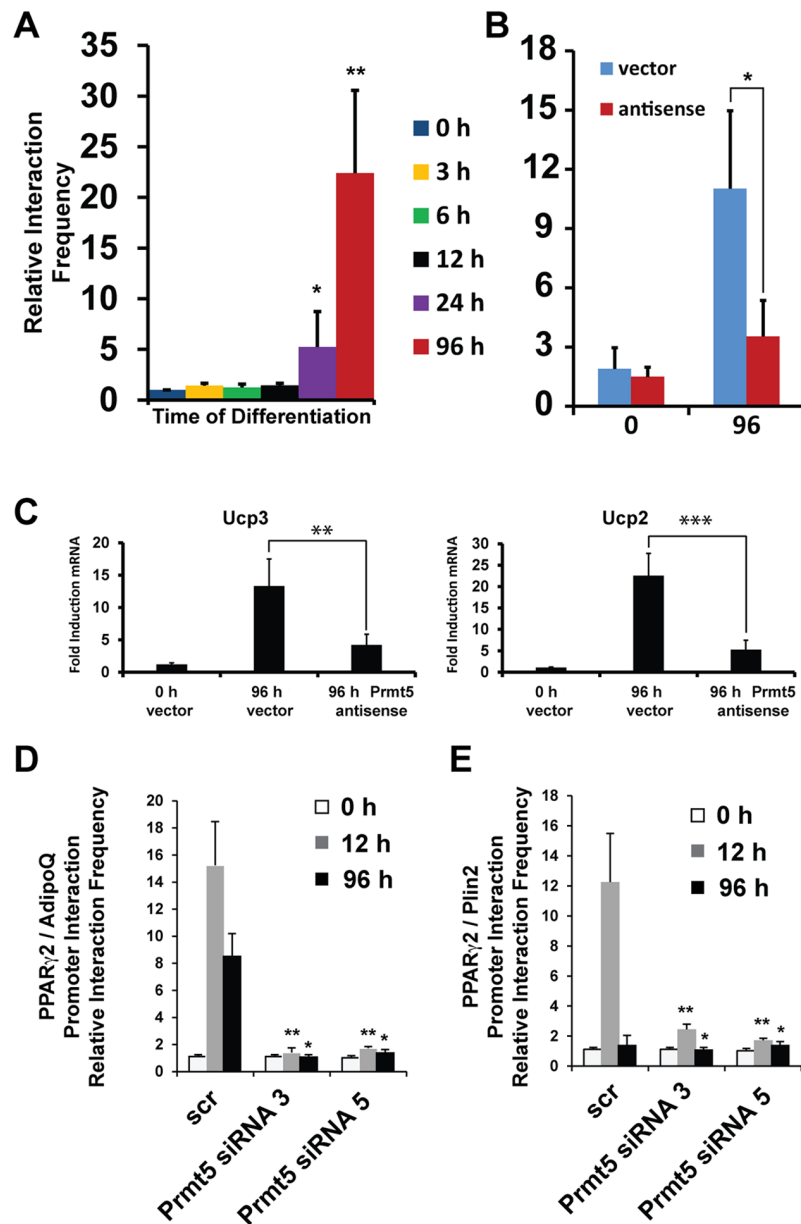


**Figure 10.** Prmt5 mediates the formation of other DNA loops and inter-chromosomal interactions during adipogenic differentiation. **(A)** Time course of relative interaction frequency between the Ucp2 and Ucp3 loci. Samples of C3H10T1/2 cells were taken at the 0 h timepoint and at 3, 6, 12, 24 and 96 h following differentiation. **(B)** Control vector and antisense Prmt5 expressing C3H10T1/2 cells either collected prior to differentiation (0 h) or 96 h later were tested by 3C for interactions between the Ucp2 and Ucp3 loci. **(C)** Control vector and antisense Prmt5 expressing C3H10T1/2 cells either collected prior to differentiation (0 h) or 96 h later were used to determine expression levels of Ucp3 and Ucp2, normalized to levels of GAPDH, by quantitative PCR. Data are presented as fold induction relative to the expression at time 0, which was set to 1. **(D and E)** Interaction frequencies between the PPAR $\gamma$ 2 promoter and the promoters of the adiponectin (AdipoQ) or perilipin 2 (Plin2) genes in C3H10T1/2 cells treated with scramble sequence (scr) siRNA or siRNAs targeting Prmt5 that were differentiated for the indicated times. All results are from three independent samples performed in triplicate. Error bars: Mean + SD (\* $P < 0.05$ , \*\* $P < 0.01$ , \*\*\* $P < 0.001$  by Student's two tailed  $t$ -test).

PPAR $\gamma$ 2 locus but also mediates other long-distance chromatin interactions both in cis and in trans during adipocyte differentiation.

## DISCUSSION

### Genomic structure of the PPAR $\gamma$ 2 locus

Three putative enhancers for the PPAR $\gamma$ 2 gene have been previously identified on the basis of chromatin signature

marks and binding by the adipogenic regulatory factors C/EBP $\beta$ , C/EBP $\alpha$  and PPAR $\gamma$ 2 (10). Two are located downstream, at 97 and 101 kb relative to the start site of transcription. The third is located ~10 kb upstream of the TSS; this sequence has been shown to drive transcription of a reporter gene in 3T3-L1 pre-adipocytes induced to differentiate (8). Here we demonstrate that this sequence modestly activates a PPAR $\gamma$ 2 reporter driven by 1.6 kb of sequence upstream of the TSS and significantly drives re-

porter gene expression in the presence of a C/EBP $\alpha$  expression vector. When we performed 3C mapping of the 80 kb upstream and the 80 kb downstream of the PPAR $\gamma$ 2 TSS using proximal promoter sequences as the anchor, the  $\sim$ 10 kb region was by far the most frequently interacting region in differentiating cells. The simplest interpretation is that a loop forms between the  $\sim$ 10 kb enhancer sequence and the proximal promoter, almost certainly for the purpose of bringing the  $\sim$ 10 kb region into close proximity to the promoter and TSS. This is, to the best of our knowledge, the first demonstration of a loop between regulatory elements at the PPAR $\gamma$ 2 locus.

While we have focused on the differentiation-dependent promoter–enhancer loop, we note that there were less frequent, but still statistically significant interactions between the PPAR $\gamma$ 2 promoter and sequences at  $\sim$ +10 kb relative to the TSS and, to an even lesser extent, between the promoter and sequences at  $\sim$ –20 to  $\sim$ –25 kb relative to the TSS. Sequence analysis of these regions does not indicate transcription factor hot spots, histone marks or DNase I hypersensitivity that would be indicative of enhancer sequences. The significance of these interactions, if any, remains to be determined. We also note that the entire locus shows a complex pattern of interactions prior to the onset of differentiation signaling and that much of this ‘structure’ does not change after the onset of differentiation. The PPAR $\gamma$ 2 promoter is contained within intron 2 of the PPAR $\gamma$ 1 gene. It is possible that much of the observed three-dimensional structure relates to higher order organization of the entire region and that differentiation-dependent induction of PPAR $\gamma$ 2 gene expression results entirely from the formation of the promoter–enhancer loop we have documented.

### Kinetics of molecular changes at the PPAR $\gamma$ 2 locus during adipogenic differentiation

Over the course of several studies, we have determined that nuclease sensitivity at the PPAR $\gamma$ 2 promoter occurs within minutes of adipogenic differentiation signaling, followed by binding of c-fos. C/EBP $\beta$  binding occurs within an hour of the onset of differentiation (51). We also determined that the PPAR $\gamma$ 2 locus subsequently makes transient, long-range intra-chromosomal as well as inter-chromosomal interactions with adipokine and other PPAR $\gamma$ 2 target genes and concluded that genome organization is dynamically remodeled in response to adipogenic signaling, perhaps for the purpose of identifying transcriptionally silent tissue-specific loci for subsequent transcriptional activation (23). All of these events required protein kinase A signaling, and elevated cyclic AMP (cAMP) levels were sufficient to induce these events even though elevated cAMP does not support completion of the adipogenic differentiation process (23,51). In the current study, we provide additional details about the molecular changes that occur at the PPAR $\gamma$ 2 locus after the onset of differentiation and coincident with expression of the PPAR $\gamma$ 2 gene. Subsequent to the transient interaction of the PPAR $\gamma$ 2 locus with several target gene loci, a loop forms between the PPAR $\gamma$ 2 promoter and an enhancer sequence 10 kb upstream of the TSS. We speculate that long-range alteration of relative adipogenic gene positioning is part of the process by which tissue specific

loci are spatially organized in the nucleus and that this more global genome organization necessarily precedes the locus-specific structural rearrangement of relevant transcriptional regulatory sequences that directly promote transcriptional activation.

### The roles of Prmt5 and MED1 in loop formation at the PPAR $\gamma$ 2 locus

Prmt5 is a methyltransferase that symmetrically dimethylates arginine residues on substrate molecules, which include histones, transcription and splicing factors, and many other proteins (52,53). We previously determined that Prmt5 is required for both myogenic and adipogenic differentiation via mechanisms that involved binding to target genes and facilitating the recruitment of the mammalian SWI/SNF chromatin remodeling enzyme (16–18), which is required for activation of differentiation-specific genes (34,54–57). In our previous report, we showed that Prmt5 was bound to the  $\sim$ 10 kb enhancer at the end point of differentiation, but could not be captured by ChIP assay on the promoter at the same time (18). In the current study, kinetic analysis of Prmt5 binding indicates that Prmt5 initiates interaction with the PPAR $\gamma$ 2 gene at promoter sequences, but this interaction is transient and cannot be seen by the time loop formation is first observed. In contrast, Prmt5 binding to the enhancer sequence gradually increases throughout the time course of differentiation and remains present after loop formation. Why binding kinetics differ as the promoter and enhancer is unclear. Prmt5 is not known to have any sequence-specific DNA binding activity and is presumed to bind via interaction with transcription factors. Perhaps Prmt5 binding to the promoter persists but steric considerations caused by loop formation prevent cross-linking between Prmt5 and the promoter sequences. Alternatively, perhaps the nucleosome structure of the PPAR $\gamma$ 2 promoter is organized in such a manner that Prmt5 interaction at the promoter leads to subsequent reorganization of chromatin structure at the enhancer. Such a model would be consistent with DNase I hypersensitivity studies indicating that increased nuclease sensitivity at the PPAR $\gamma$ 2 promoter precedes increased nuclease sensitivity at the  $\sim$ 10 kb enhancer (9). Another possibility is that Prmt5 binding at different times and locations indicate separable functions. Prmt5 binding at the promoter correlates with the timing of the inter- and long-range intra-chromosomal interactions between the PPAR $\gamma$ 2 promoter and other adipogenic loci (23). Since Prmt5 binding promotes interaction of SWI/SNF chromatin remodeling enzymes with the chromatin (16–18) and it has been documented that the Brg1 ATPase of mammalian SWI/SNF chromatin remodeling enzymes mediates both locus-specific chromatin reorganization (35,37,39,40) as well as formation of inter-chromosomal interactions in other differentiation systems (58), perhaps binding of Prmt5, and, by extension, targeting SWI/SNF enzyme to the promoter, is part of the mechanism by which the inter- and long-range intra-chromosomal interactions between the PPAR $\gamma$ 2 locus and target gene loci are facilitated.

The connection between Prmt5 and loop formation established by our kinetic analyses of Prmt5 binding, loop for-

mation and PPAR $\gamma$ 2 expression is solidified by our demonstration that Prmt5 knockdown prevents all three of these events and that Prmt5 overexpression causes premature loop formation and early expression of PPAR $\gamma$ 2. Further investigation centered on Mediator complex, which is a large, multi-subunit cofactor of RNA polymerase II that facilitates activator-mediated transcription (41,59). Mediator subunits were long ago recognized as essential molecular components of the adipogenic gene expression and differentiation processes (42,60,61), and Mediator, in conjunction with cohesion, were determined to physically connect enhancers and promoters (62). More recently, detailed analyses of the three-dimensional structural organization of multiple loci in ES cells programmed to differentiate along the neuro-ectodermal lineage showed that a Mediator-cohesin complex bridges short-range enhancer-promoter connections and that knockdown of Mediator subunits disrupted the spatial architecture of the examined loci (63). We determined that Mediator interacts constitutively with the PPAR $\gamma$ 2 upstream enhancer and inducibly at the promoter, matching the kinetics of Prmt5 promoter binding. A schematic model of the molecular changes that occur at the PPAR $\gamma$ 2 promoter is presented in Supplemental Figure S5.

Consistent with expectations based on the literature, knockdown of Mediator subunit MED1 inhibited differentiation and greatly reduced loop formation. Perhaps not surprisingly, MED1 knockdown also prevented Prmt5 and SWI/SNF enzyme binding. It is known that both Brg1 and Prmt5 interact with the CDK proteins of the Mediator complex in other biological contexts (44,64). Additionally, the loss of the CDK proteins in Mediator prevented interaction with Prmt5 and loss of Prmt5 binding at C/EBP $\beta$  target genes during immune responses, suggesting interplay between the factors (44). Thus the observation of loss of Prmt5 and Brg1 binding upon MED1 knockdown supports and extends the previous findings.

What was unexpected was the observation that MED1 and Prmt5 show mutual dependency for binding to the PPAR $\gamma$ 2, as Prmt5 knockdown significantly reduced Mediator binding. This observation suggests that Mediator and Prmt5 may be recruited while as part of a complex in a manner that requires the integrity of both components. Similarly, the integrity of both components presumably would then be required for promoter-enhancer loop formation at the PPAR $\gamma$ 2 locus. The exact nature of the mutual dependency between Prmt5 and Mediator remains to be determined, but the links between the two presented here and in other biological systems suggest that combined functionality is a general occurrence.

### Pleiotropic Prmt5 functions

Here we report that Prmt5 facilitates promoter-enhancer looping and gene expression at the PPAR $\gamma$ 2 locus, which encodes a critical lineage-determining factor that drives the differentiation of adipose tissue. In addition, we report that Prmt5 mediates long-range, inter-chromosomal interactions involving the PPAR $\gamma$  locus as well as looping interactions between gene loci expressed during adipogenesis. These data suggest that Prmt5 may be broadly required for the formation of higher-order chromatin interactions

during adipocyte differentiation, although the global extent of this Prmt5 requirement remains to be determined. This novel Prmt5 function adds organization of higher-order chromatin structure to a long list of properties attributed to Prmt5. Prmt5 is essential for early embryonic viability and epiblast differentiation (12), marking it as an essential developmental regulator. It is found in both the nucleus and cytoplasm (65) and has been implicated in not just transcriptional regulation and control of chromatin modification but also in signal transduction, both at the cell membrane as well as in the cytosol, splicing, glucose metabolism and the DNA damage response (66–71). Prmt5 itself has associated cofactors with which it interacts, including Mep50, which is required for many Prmt5 functions (72,73), Rio Kinase 1 and ICLN, which antagonistically regulate Prmt5 substrate specificity in the cytoplasm and may implicate Prmt5 in rRNA processing (74,75), COPR5, which regulates specificity of histone methylation and can promote the transition between precursor cell and differentiation (68,75,76), and HSP90, which promotes protein stability (77). All of these functions likely impact the progression of a differentiation pathway. The ever-growing data indicate that Prmt5 plays a significant role in multiple molecular events governing development, cell proliferation and metabolism, genome organization, and gene expression, thereby implicating it as a general regulator of cellular function.

### SUPPLEMENTARY DATA

Supplementary Data are available at NAR Online.

### ACKNOWLEDGEMENT

We thank AR Barutcu and H Xiao for technical assistance and advice.

### FUNDING

National Institutes of Health (NIH) [DK084278 to S.S., A.N.I., GM56244 to A.N.I., F32DK082263 to S.E.L., DK32520 to UMass Medical School Diabetes and Endocrine Research Center]. Funding for open access charge: Institutional funds.

*Conflict of interest statement.* None declared.

### REFERENCES

- Rosen, E.D. and MacDougald, O.A. (2006) Adipocyte differentiation from the inside out. *Nat. Rev. Mol. Cell. Biol.*, **7**, 885–896.
- Farmer, S.R. (2006) Transcriptional control of adipocyte formation. *Cell Metab.*, **4**, 263–273.
- Siersbaek, R., Baek, S., Rabiee, A., Nielsen, R., Traynor, S., Clark, N., Sandelin, A., Jensen, O.N., Sung, M.-H., Hager, G.L. *et al.* (2014) Molecular architecture of transcription factor hotspots in early adipogenesis. *Cell Rep.*, **7**, 1434–1442.
- Siersbaek, R., Baek, S., Rabiee, A., Nielsen, R., Traynor, S., Clark, N., Sandelin, A., Jensen, O.N., Sung, M.-H., Hager, G.L. *et al.* (2014) Molecular architecture of transcription factor hotspots in early adipogenesis. *Cell Rep.*, **7**, 1434–1442.
- Lefterova, M.I. and Lazar, M.A. (2009) New developments in adipogenesis. *Trends Endocrinol. Metab.*, **20**, 107–114.
- Lefterova, M.I., Zhang, Y., Steger, D.J., Schupp, M., Schug, J., Cristancho, A., Feng, D., Zhuo, D., Stoeckert Jr, C.J., Liu, X.S. *et al.* (2008) PPARgamma and C/EBP factors orchestrate adipocyte

- biology via adjacent binding on a genome-wide scale. *Genes Dev.*, **22**, 2941–2952.
7. Nolis, I.K., McKay, D.J., Mantouvalou, E., Lomvardas, S., Merika, M. and Thanos, D. (2009) Transcription factors mediate long-range enhancer-promoter interactions. *Proc. Natl. Acad. Sci. U.S.A.*, **106**, 20222–20227.
  8. Steger, D.J., Grant, G.R., Schupp, M., Tomaru, T., Lefterova, M.I., Schug, J., Manduchi, E., Stoeckert, C.J. and Lazar, M.A. (2010) Propagation of adipogenic signals through an epigenomic transition state. *Genes Dev.*, **24**, 1035–1044.
  9. Siersbaek, R., Nielsen, R., John, S., Sung, M.H., Baek, S., Loft, A., Hager, G.L. and Mandrup, S. (2011) Extensive chromatin remodelling and establishment of transcription factor ‘hotspots’ during early adipogenesis. *EMBO J.*, **30**, 1459–1472.
  10. Lee, J.-E., Wang, C., Xu, S., Cho, Y.-W., Wang, L., Feng, X., Baldridge, A., Sartorelli, V., Zhuang, L., Peng, W. *et al.* (2013) H3K4 mono- and di-methyltransferase MLL4 is required for enhancer activation during cell differentiation. *Life*, **2**, e01503.
  11. Siersbaek, R., Rabiee, A., Nielsen, R., Sidoli, S., Traynor, S., Loft, A., La Cour Poulsen, L., Rogowska-Wrzesinska, A., Jensen, O.N. and Mandrup, S. (2014) Transcription factor cooperativity in early adipogenic hotspots and super-enhancers. *Cell Rep.*, **7**, 1443–1455.
  12. Tee, W.W., Pardo, M., Theunissen, T.W., Yu, L., Choudhary, J.S., Hajkova, P. and Surani, M.A. (2010) Prmt5 is essential for early mouse development and acts in the cytoplasm to maintain ES cell pluripotency. *Genes Dev.*, **24**, 2772–2777.
  13. Fabbriozzi, E., El Messaoudi, S., Polanowska, J., Paul, C., Cook, J.R., Lee, J.H., Negre, V., Rousset, M., Pestka, S., Le Cam, A. *et al.* (2002) Negative regulation of transcription by the type II arginine methyltransferase PRMT5. *EMBO Rep.*, **3**, 641–645.
  14. Pal, S., Vishwanath, S.N., Erdjument-Bromage, H., Tempst, P. and Sif, S. (2004) Human SWI/SNF-associated PRMT5 methylates histone H3 arginine 8 and negatively regulates expression of ST7 and NM23 tumor suppressor genes. *Mol. Cell. Biol.*, **24**, 9630–9645.
  15. Wei, H., Mundade, R., Lange, K.C. and Lu, T. (2014) Protein arginine methylation of non-histone proteins and its role in diseases. *Cell Cycle*, **13**, 32–41.
  16. Dacwag, C.S., Bedford, M.T., Sif, S. and Imbalzano, A.N. (2009) Distinct protein arginine methyltransferases promote ATP-dependent chromatin remodeling function at different stages of skeletal muscle differentiation. *Mol. Cell. Biol.*, **29**, 1909–1921.
  17. Dacwag, C.S., Ohkawa, Y., Pal, S., Sif, S. and Imbalzano, A.N. (2007) The protein arginine methyltransferase Prmt5 is required for myogenesis because it facilitates ATP-dependent chromatin remodeling. *Mol. Cell. Biol.*, **27**, 384–394.
  18. LeBlanc, S.E., Konda, S., Wu, Q., Hu, Y.-J., Osowski, C.M., Sif, S. and Imbalzano, A.N. (2012) Protein arginine methyltransferase 5 (Prmt5) promotes gene expression of peroxisome proliferator-activated receptor  $\gamma$ 2 (PPAR $\gamma$ 2) and its target genes during adipogenesis. *Mol. Endocrinol.*, **26**, 583–597.
  19. Dekker, J., Rippe, K., Dekker, M. and Kleckner, N. (2002) Capturing chromosome conformation. *Science*, **295**, 1306–1311.
  20. Osborne, C.S., Chakalova, L., Brown, K.E., Carter, D., Horton, A., Debrand, E., Goyenechea, B., Mitchell, J.A., Lopes, S., Reik, W. *et al.* (2004) Active genes dynamically colocalize to shared sites of ongoing transcription. *Nat. Genet.*, **36**, 1065–1071.
  21. Sexton, T., Kurukuti, S., Mitchell, J.A., Umlauf, D., Nagano, T. and Fraser, P. (2012) Sensitive detection of chromatin coassociations using enhanced chromosome conformation capture on chip. *Nat. Protoc.*, **7**, 1335–1350.
  22. Palstra, R.J., Tolhuis, B., Splinter, E., Nijmeijer, R., Grosveld, F. and de Laat, W. (2003) The beta-globin nuclear compartment in development and erythroid differentiation. *Nat. Genet.*, **35**, 190–194.
  23. LeBlanc, S.E., Wu, Q., Barutcu, A.R., Xiao, H., Ohkawa, Y. and Imbalzano, A.N. (2014) The PPAR $\gamma$  locus makes long-range chromatin interactions with selected tissue-specific gene loci during adipocyte differentiation in a protein kinase A dependent manner. *PLoS One*, **9**, e86140.
  24. Pal, S., Yun, R., Datta, A., Lacomis, L., Erdjument-Bromage, H., Kumar, J., Tempst, P. and Sif, S. (2003) mSin3A/histone deacetylase 2- and PRMT5-containing Brg1 complex is involved in transcriptional repression of the Myc target gene cad. *Mol. Cell. Biol.*, **23**, 7475–7487.
  25. Pear, W.S., Nolan, G.P., Scott, M.L. and Baltimore, D. (1993) Production of high-titer helper-free retroviruses by transient transfection. *Proc. Natl. Acad. Sci. U.S.A.*, **90**, 8392–8396.
  26. Schmittgen, T.D. and Livak, K.J. (2008) Analyzing real-time PCR data by the comparative C(T) method. *Nat. Protoc.*, **3**, 1101–1108.
  27. de La Serna, I.L., Carlson, K.A., Hill, D.A., Guidi, C.J., Stephenson, R.O., Sif, S., Kingston, R.E. and Imbalzano, A.N. (2000) Mammalian SWI-SNF complexes contribute to activation of the hsp70 gene. *Mol. Cell. Biol.*, **20**, 2839–2851.
  28. Gill, G. and Ptashne, M. (1988) Negative effect of the transcriptional activator GAL4. *Nature*, **334**, 721–724.
  29. Bartkuhn, M. and Renkawitz, R. (2008) Long range chromatin interactions involved in gene regulation. *Biochim. Biophys. Acta*, **1783**, 2161–2166.
  30. Harms, M.J., Lim, H.-W., Ho, Y., Shapira, S.N., Ishibashi, J., Rajakumari, S., Steger, D.J., Lazar, M.A., Won, K.-J. and Seale, P. (2015) PRDM16 binds MED1 and controls chromatin architecture to determine a brown fat transcriptional program. *Genes Dev.*, **29**, 298–307.
  31. Iida, S., Chen, W., Nakadai, T., Ohkuma, Y. and Roeder, R.G. (2015) PRDM16 enhances nuclear receptor-dependent transcription of the brown fat-specific Ucp1 gene through interactions with Mediator subunit MED1. *Genes Dev.*, **29**, 308–321.
  32. Bugge, A., Siersbaek, M., Madsen, M.S., Gondor, A., Rougier, C. and Mandrup, S. (2010) A novel intronic peroxisome proliferator-activated receptor gamma enhancer in the uncoupling protein (UCP) 3 gene as a regulator of both UCP2 and -3 expression in adipocytes. *J. Biol. Chem.*, **285**, 17310–17317.
  33. Dekker, J. (2006) The three ‘C’ s of chromosome conformation capture: controls, controls, controls. *Nat. Methods*, **3**, 17–21.
  34. Salma, N., Xiao, H., Mueller, E. and Imbalzano, A.N. (2004) Temporal recruitment of transcription factors and SWI/SNF chromatin-remodeling enzymes during adipogenic induction of the peroxisome proliferator-activated receptor gamma nuclear hormone receptor. *Mol. Cell. Biol.*, **24**, 4651–4663.
  35. Kim, S.I., Bresnick, E.H. and Bultman, S.J. (2009) BRG1 directly regulates nucleosome structure and chromatin looping of the alpha globin locus to activate transcription. *Nucleic Acids Res.*, **37**, 6019–6027.
  36. Kim, S.I., Bultman, S.J., Jing, H., Blobel, G.A. and Bresnick, E.H. (2007) Dissecting molecular steps in chromatin domain activation during hematopoietic differentiation. *Mol. Cell. Biol.*, **27**, 4551–4565.
  37. Kim, S.I., Bultman, S.J., Kiefer, C.M., Dean, A. and Bresnick, E.H. (2009) BRG1 requirement for long-range interaction of a locus control region with a downstream promoter. *Proc. Natl. Acad. Sci. U.S.A.*, **106**, 2259–2264.
  38. Bossen, C., Murre, C.S., Chang, A.N., Mansson, R., Rodewald, H.R. and Murre, C. (2015) The chromatin remodeler Brg1 activates enhancer repertoires to establish B cell identity and modulate cell growth. *Nat. Immunol.*, **16**, 775–784.
  39. Cai, S., Lee, C.C. and Kohwi-Shigematsu, T. (2006) SATB1 packages densely looped, transcriptionally active chromatin for coordinated expression of cytokine genes. *Nat. Genet.*, **38**, 1278–1288.
  40. Ni, Z., Abou El Hassan, M., Xu, Z., Yu, T. and Bremner, R. (2008) The chromatin-remodeling enzyme BRG1 coordinates CIITA induction through many interdependent distal enhancers. *Nat. Immunol.*, **9**, 785–793.
  41. Allen, B.L. and Taatjes, D.J. (2015) The mediator complex: a central integrator of transcription. *Nat. Rev. Mol. Cell. Biol.*, **16**, 155–166.
  42. Ge, K., Guermah, M., Yuan, C.-X., Ito, M., Wallberg, A.E., Spiegelman, B.M. and Roeder, R.G. (2002) Transcription coactivator TRAP220 is required for PPAR gamma 2-stimulated adipogenesis. *Nature*, **417**, 563–567.
  43. Carlsten, J.O., Zhu, X. and Gustafsson, C.M. (2013) The multitasked Mediator complex. *Trends Biochem. Sci.*, **38**, 531–537.
  44. Tsutsui, T., Fukasawa, R., Shinmyozu, K., Nakagawa, R., Tobe, K., Tanaka, A. and Ohkuma, Y. (2013) Mediator complex recruits epigenetic regulators via its two cyclin-dependent kinase subunits to repress transcription of immune response genes. *J. Biol. Chem.*, **288**, 20955–20965.
  45. Fleury, C., Neverova, M., Collins, S., Raimbault, S., Champigny, O., Levi-Meyrueis, C., Bouillaud, F., Seldin, M.F., Surwit, R.S., Ricquier, D. *et al.* (1997) Uncoupling protein-2: a novel gene linked to obesity and hyperinsulinemia. *Nat. Genet.*, **15**, 269–272.

46. Gong, D.W., He, Y., Karas, M. and Reitman, M. (1997) Uncoupling protein-3 is a mediator of thermogenesis regulated by thyroid hormone, beta3-adrenergic agonists, and leptin. *J. Biol. Chem.*, **272**, 24129–24132.
47. Jaburek, M., Varecha, M., Gimeno, R.E., Dembski, M., Jezek, P., Zhang, M., Burn, P., Tartaglia, L.A. and Garlid, K.D. (1999) Transport function and regulation of mitochondrial uncoupling proteins 2 and 3. *J. Biol. Chem.*, **274**, 26003–26007.
48. Arsenijevic, D., Onuma, H., Pecqueur, C., Raimbault, S., Manning, B.S., Miroux, B., Couplan, E., Alves-Guerra, M.C., Goubern, M., Surwit, R. *et al.* (2000) Disruption of the uncoupling protein-2 gene in mice reveals a role in immunity and reactive oxygen species production. *Nat. Genet.*, **26**, 435–439.
49. Bouillaud, F. (2009) UCP2, not a physiologically relevant uncoupler but a glucose sparing switch impacting ROS production and glucose sensing. *Biochim. Biophys. Acta*, **1787**, 377–383.
50. Pi, J., Bai, Y., Daniel, K.W., Liu, D., Lyght, O., Edelstein, D., Brownlee, M., Corkey, B.E. and Collins, S. (2009) Persistent oxidative stress due to absence of uncoupling protein 2 associated with impaired pancreatic beta-cell function. *Endocrinology*, **150**, 3040–3048.
51. Xiao, H., Leblanc, S.E., Wu, Q., Konda, S., Salma, N., Marfella, C.G.A., Ohkawa, Y. and Imbalzano, A.N. (2011) Chromatin accessibility and transcription factor binding at the PPAR $\gamma$ 2 promoter during adipogenesis is protein kinase A-dependent. *J. Cell. Physiol.*, **226**, 86–93.
52. Di Lorenzo, A. and Bedford, M.T. (2011) Histone arginine methylation. *FEBS Lett.*, **585**, 2024–2031.
53. Yang, Y. and Bedford, M.T. (2013) Protein arginine methyltransferases and cancer. *Nat. Rev. Cancer*, **13**, 37–50.
54. de la Serna, I.L., Carlson, K.A. and Imbalzano, A.N. (2001) Mammalian SWI/SNF complexes promote MyoD-mediated muscle differentiation. *Nat. Genet.*, **27**, 187–190.
55. de la Serna, I.L., Ohkawa, Y., Berkes, C.A., Bergstrom, D.A., Dacwag, C.S., Tapscott, S.J. and Imbalzano, A.N. (2005) MyoD targets chromatin remodeling complexes to the myogenin locus prior to forming a stable DNA-bound complex. *Mol. Cell. Biol.*, **25**, 3997–4009.
56. de la Serna, I.L., Ohkawa, Y., Higashi, C., Dutta, C., Osias, J., Kommasjyula, N., Tachibana, T. and Imbalzano, A.N. (2006) The microphthalmia-associated transcription factor (MITF) requires SWI/SNF enzymes to activate melanocyte specific genes. *J. Biol. Chem.*, **281**, 20233–20241.
57. Pedersen, T.A., Kowenz-Leutz, E., Leutz, A. and Nerlov, C. (2001) Cooperation between C/EBP $\alpha$  TBP/TFIIB and SWI/SNF recruiting domains is required for adipocyte differentiation. *Genes Dev.*, **15**, 3208–3216.
58. Harada, A., Mallappa, C., Okada, S., Butler, J.T., Baker, S.P., Lawrence, J.B., Ohkawa, Y. and Imbalzano, A.N. (2015) Spatial re-organization of myogenic regulatory sequences temporally controls gene expression. *Nucleic Acids Res.*, **43**, 2008–2021.
59. Poss, Z.C., Ebmeier, C.C. and Taatjes, D.J. (2013) The Mediator complex and transcription regulation. *Crit. Rev. Biochem. Mol. Biol.*, **48**, 575–608.
60. Ge, K., Cho, Y.W., Guo, H., Hong, T.B., Guermah, M., Ito, M., Yu, H., Kalkum, M. and Roeder, R.G. (2008) Alternative mechanisms by which mediator subunit MED1/TRAP220 regulates peroxisome proliferator-activated receptor gamma-stimulated adipogenesis and target gene expression. *Mol. Cell. Biol.*, **28**, 1081–1091.
61. Yang, W., Rachez, C. and Freedman, L.P. (2000) Discrete roles for peroxisome proliferator-activated receptor gamma and retinoid X receptor in recruiting nuclear receptor coactivators. *Mol. Cell. Biol.*, **20**, 8008–8017.
62. Kagey, M.H., Newman, J.J., Bilodeau, S., Zhan, Y., Orlando, D.A., van Berkum, N.L., Ebmeier, C.C., Goossens, J., Rahl, P.B., Levine, S.S. *et al.* (2010) Mediator and cohesin connect gene expression and chromatin architecture. *Nature*, **467**, 430–435.
63. Phillips-Cremins, J.E., Sauria, M.E., Sanyal, A., Gerasimova, T.I., Lajoie, B.R., Bell, J.S., Ong, C.T., Hookway, T.A., Guo, C., Sun, Y. *et al.* (2013) Architectural protein subclasses shape 3D organization of genomes during lineage commitment. *Cell*, **153**, 1281–1295.
64. Fukasawa, R., Tsutsui, T., Hirose, Y., Tanaka, A. and Ohkuma, Y. (2012) Mediator CDK subunits are platforms for interactions with various chromatin regulatory complexes. *J. Biochem.*, **152**, 241–249.
65. Gu, Z., Li, Y., Lee, P., Liu, T., Wan, C. and Wang, Z. (2012) Protein arginine methyltransferase 5 functions in opposite ways in the cytoplasm and nucleus of prostate cancer cells. *PLoS One*, **7**, e44033.
66. Jansson, M., Durant, S.T., Cho, E.C., Sheahan, S., Edelmann, M., Kessler, B. and Thangue, N.B. (2008) Arginine methylation regulates the p53 response. *Nat. Cell Biol.*, **10**, 1431–1439.
67. Kanamalluru, D., Xiao, Z., Fang, S., Choi, S.E., Kim, D.H., Veenstra, T.D. and Kemper, J.K. (2011) Arginine methylation by PRMT5 at a naturally occurring mutation site is critical for liver metabolic regulation by small heterodimer partner. *Mol. Cell. Biol.*, **31**, 1540–1550.
68. Paul, C., Sardet, C. and Fabbriozzi, E. (2015) The Wnt-target gene Dlk-1 is regulated by the Prmt5-associated factor Copr5 during adipogenic conversion. *Biol. Open*, **4**, 312–316.
69. Pesiridis, G.S., Diamond, E. and Duyne, G.D. (2009) Role of pICln in methylation of Sm proteins by PRMT5. *J. Biol. Chem.*, **284**, 21347–21359.
70. Sun, L., Wang, M., Lv, Z., Yang, N., Liu, Y., Bao, S., Gong, W. and Xu, R.M. (2011) Structural insights into protein arginine symmetric dimethylation by PRMT5. *Proc. Natl. Acad. Sci. U.S.A.*, **108**, 20538–20543.
71. Tsai, W.-W., Niessen, S., Goebel, N., Yates, J.R., Guccione, E. and Montminy, M. (2013) PRMT5 modulates the metabolic response to fasting signals. *Proc. Natl. Acad. Sci. U.S.A.*, **110**, 8870–8875.
72. Aggarwal, P., Vaites, L.P., Kim, J.K., Mellert, H., Gurung, B., Nakagawa, H., Herlyn, M., Hua, X., Rustgi, A.K., McMahon, S.B. *et al.* (2010) Nuclear cyclin D1/CDK4 kinase regulates CUL4 expression and triggers neoplastic growth via activation of the PRMT5 methyltransferase. *Cancer Cell*, **18**, 329–340.
73. Friesen, W.J., Wyce, A., Paushkin, S., Abel, L., Rappsilber, J., Mann, M. and Dreyfuss, G. (2002) A novel WD repeat protein component of the methylosome binds Sm proteins. *J. Biol. Chem.*, **277**, 8243–8247.
74. Guderian, G., Peter, C., Wiesner, J., Sickmann, A., Schulze-Osthoff, K., Fischer, U. and Grimmer, M. (2011) RioK1, a new interactor of protein arginine methyltransferase 5 (PRMT5), competes with pICln for binding and modulates PRMT5 complex composition and substrate specificity. *J. Biol. Chem.*, **286**, 1976–1986.
75. LaRonde-LeBlanc, N. and Wlodawer, A. (2005) A family portrait of the RIO kinases. *J. Biol. Chem.*, **280**, 37297–37300.
76. Paul, C., Sardet, C. and Fabbriozzi, E. (2012) The histone- and PRMT5-associated protein COPR5 is required for myogenic differentiation. *Cell Death Differ.*, **19**, 900–908.
77. Maloney, A., Clarke, P.A., Naaby-Hansen, S., Stein, R., Koopman, J.O., Akpan, A., Yang, A., Zvelebil, M., Cramer, R., Stimson, L. *et al.* (2007) Gene and protein expression profiling of human ovarian cancer cells treated with the heat shock protein 90 inhibitor 17-allylamino-17-demethoxygeldanamycin. *Cancer Res.*, **67**, 3239–3253.